HYDROGEN SEPARATION MEMBRANES FOR VISION 21 FOSSIL FUEL PLANTS

Shane E. Roark, Richard Mackay, Anthony F. Sammells

Eltron Research Inc.
4600 Nautilus Court South
Boulder, CO 80301-3241

Phone: (303) 530-0263
Fax: (303) 530-0264
eltron@eltronresearch.com
www.eltronresearch.com

ABSTRACT

Eltron Research and team members CoorsTek, McDermott Technology, Süd Chemie, Argonne National Laboratory, and Oak Ridge National Laboratory are developing an environmentally benign, inexpensive, and efficient method for separating hydrogen from gas mixtures produced during industrial processes, such as coal gasification. This objective is being pursued using dense membranes based in part on Eltron-patented ceramic materials with a demonstrated ability for proton and electron conduction. The technical goals are being addressed by modifying single-phase and composite membrane composition and microstructure to maximize proton and electron conductivity without loss of material stability. Ultimately, these materials must enable hydrogen separation at practical rates under ambient and high-pressure conditions, without deactivation in the presence of feedstream components such as carbon dioxide, water, and sulfur.

This project was motivated by the Department of Energy (DOE) National Energy Technology Laboratory (NETL) Vision 21 initiative which seeks to economically eliminate environmental concerns associated with the use of fossil fuels. The proposed technology addresses the DOE Vision 21 initiative in two ways. First, this process offers a relatively inexpensive solution for pure hydrogen separation that can be easily incorporated into Vision 21 fossil fuel plants. Second, this process could reduce the cost of hydrogen, which is a clean burning fuel under increasing demand as supporting technologies are developed for hydrogen utilization and storage. Additional motivation for this project arises from the potential of this technology for other applications. By appropriately changing the catalysts coupled with the membrane, essentially the same system can be used to facilitate alkane dehydrogenation and coupling, aromatics processing, and hydrogen sulfide decomposition.

INTRODUCTION

Since the discovery in the early 1980s by Iwahara *et al.* of high temperature proton conduction in $SrCeO_3$, perovskite-based oxides have been the focus of extensive studies.[1-3] The potential for these materials in fuel cells and chemical sensors was quickly recognized and the majority of work has thus focused on achieving high proton conductivity without electron/hole conduction. After nearly twenty years of rigorous investigations, it has been determined that the highest level of proton conductivity is achieved by selectively doping perovskites, such as cerates and zirconates of Ba and Sr. In particular, $SrCeO_3$ and $BaCeO_3$ doped with trivalent cations such as Y, Yb, and Gd have been identified as particularly good high-temperature proton conductors.[2,4-9]

The general formula for these materials can be represented as ABO_3, or for doped perovskites $A_{1-x}A_x'B_{1-y}B_y'O_{3-\delta}$, where x and y are the fractions of dopants in the A and B sites, respectively, and δ is the number of oxygen vacancies. Doping the B site with lower valence cations produces oxygen vacancies to maintain electroneutrality, and the presence of oxygen vacancies is necessary for maximum proton conduction. The quantity of proton charge carriers that can be introduced into a given material is dependent on the dopant concentration, the number of oxygen vacancies, the atmospheric conditions, and temperature.[4,10] For doped $BaCeO_3$ materials, proton concentrations from less than 0.1 mol% to greater than 10 mol% can be achieved depending on the exact composition, and operation conditions.[4,11-14] The result of the increased charge carrier concentration arising from doping these perovskite materials is an increase in proton conductivity between two and four orders of magnitude relative to the undoped analogs.

For dense membranes to transport hydrogen they also must have high electron conductivity. Accordingly, much of the recent work developing ceramic materials for hydrogen separation has focused on introducing electron conductivity to high-temperature proton conductors. For example, Balachandran *et al.* investigated the proton conductor Y-doped $BaCeO_3$.[15,16] Despite relatively high proton conductivity, the electronic conductivity was low and an applied current density of 50 mA/cm^2 was necessary to transport hydrogen at a rate of ~0.25 mL/min/cm^2 (mL of hydrogen per minute per cm^2 of membrane surface). However, by incorporating an electron conducting second phase, a comparable hydrogen transport rate was achieved in the non-galvanic mode.[16] Similar results were obtained at Eltron using cerates doped with transition metals to impart electronic conductivity.[17]

The process for hydrogen separation using a dense ceramic-based membrane is shown schematically in Figure 1. In this example, a syngas mixture (H_2, CO, and CO_2) is passed across the membrane surface where hydrogen is oxidized catalytically. The protons and electrons generated are incorporated into the membrane material lattice and conducted to the reduction surface where the reverse reduction reaction occurs to produce pure hydrogen. Provided practical hydrogen separation rates can be achieved with derivatives of these ceramic materials, it is anticipated that the mature technology will offer the following advantages over alternative separation methods: i) The membrane materials are relatively inexpensive and the system design is inherently simple, requiring no external circuitry or applied potential. ii) Since the membranes are nonporous, only hydrogen is transported without contributions from break-through of other gases. Accordingly, secondary purification steps are not necessary, and membranes are not subject to problems associated with pore clogging. iii) The transport mechanism in these materials occurs at temperatures compatible with incorporation into chemical processing

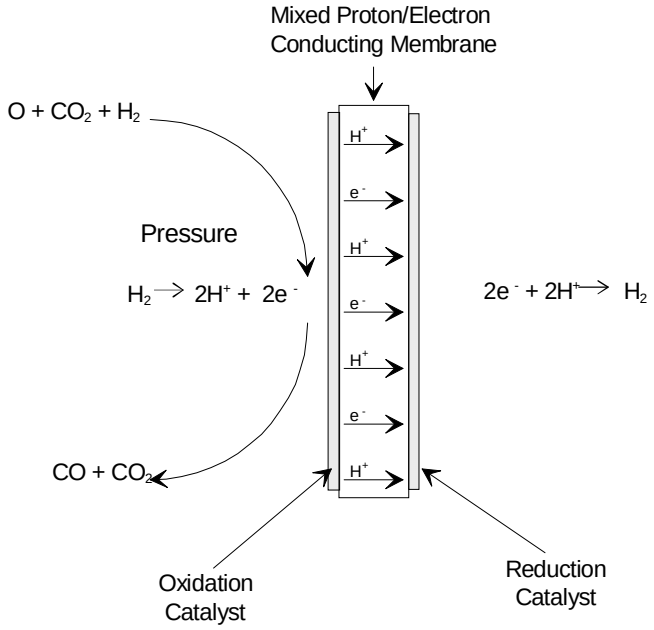

Figure 1. Schematic diagram of the ceramic membrane process for separating hydrogen from a mixture of gases.

streams. iv) The membrane system is highly versatile and can be used to facilitate numerous chemical processing applications by appropriately adjusting the catalysts.

TRANSPORT PROCESS IN DENSE CERAMIC MEMBRANES

The introduction of protons into the perovskite ceramic generally is shown in terms of moisture containing gas streams as an acid/base equilibrium between water molecules and oxygen vacancies. Using Kröger-Vink notation,[18] oxygen vacancies, $V_o^{\cdot\cdot}$, react with water to fill lattice positions with oxide ions, $O_o^{\times}$, and produce interstitial protons, $H_i^{\cdot}$, according to,[4]

$$H_2O + V_o^{\cdot\cdot} \leftrightarrows O_o^{\times} + 2H_i^{\cdot}. \quad (1)$$

Protons are retained in the material by associating with oxide ions at normal lattice sites,

$$O_o^{\times} + H_i^{\cdot} = OH_o^{\cdot} \quad (2)$$

so that the net reaction demonstrating the interaction of oxygen vacancies with water vapor to produce proton charge carriers can be written as,

$$H_2O + V_o^{\cdot\cdot} + O_o^{\times} \leftrightarrows 2OH_o^{\cdot}. \quad (3)$$

However, in the absence of moisture, hydrogen in the gas stream is incorporated directly into the material as protons and electrons (e´) through interaction with oxide ions according to,

$$\tfrac{1}{2} H_2 + O_o^{\times} \leftrightarrows OH_o^{\cdot} + e'. \quad (4)$$

Alternatively, an analogous equation can be written in terms of hole conduction as well.

Conduction of protons and electrons across the ceramic membrane is driven by the conditions or processes occurring at opposite surfaces of the membrane. For hydrogen separation, the driving force is a concentration gradient corresponding to a Nernstian potential difference between 50 and 500 mV, dictated in part by the ratio of hydrogen partial pressure on opposite sides of the membrane. This potential difference determines the rate of conduction up to the catalysis-, mass transfer-, or material-limited rate.

It is generally accepted that once protons are incorporated into the material, they are conducted by transference between oxygen ions at normal lattice positions.[4,11-13] However, arguments have been presented for OH^- conduction as well.[4,11-13] It is possible that both mechanisms occur to some extent, and the relative contributions to overall proton conductivity will be dependent on the material composition, the operation temperature, and gas stream composition. Numerous techniques have been employed to determine the dominant charge carrier in perovskite materials, and the conclusion of proton "hopping" at moderate temperatures (less than ~800°C) is based on i) isotope effect studies that demonstrate the predicted $\sqrt{2}$ factor greater conductivity for protons than deuterium ions,[6,10] ii) chemical analysis of the product effluents from electrochemical cells under DC conditions,[2,10,19,20] iii) comparison of measured and theoretical potentials from hydrogen and steam concentration cells,[5,21,22] and iv) ^{18}O diffusivity experiments that largely rule out OH^- transport.[10]

It also has been observed that the activation energy for proton conduction decreases, and the proton mobility increases when the distance between oxygen ions in the lattice is increased.[10] Based on this result, and the fact that typical activation energies are too low to support proton jumping between static oxygen sites, it has been proposed that thermal fluctuations of oxygen ions facilitate proton transfer.[23] As oxygen anions move closer together during a vibration, the energy barrier for

proton transfer diminishes. This description of the conduction mechanism has been cited to explain the low activation energies and high proton mobilities for loose-packed structures with soft metal-oxygen bonds.[4]

Support for this explanation is derived from quantum molecular dynamic simulations of proton conduction in $BaCeO_3$, $BaTiO_3$, and $BaZrO_3$.[24,25] From these simulations, the critical factors that influence conductivity were suggested to be the degree of covalence between B site cations and oxygen anions, and the degree of hydrogen bonding within the lattice.[24,25] Materials with relatively open crystal structures have greater separation between oxygen anions and a tendency for low B-O covalence. The low covalence results in softer B-O vibrations that facilitate transfer of protons between oxygen sites. Thus, the potential barrier for proton transfer oscillates between high and low values with the molecular vibration as the separation between oxygen anions fluctuates. It also is expected that a high degree of hydrogen bonding leads to greater proton conduction since, in this case, protons are somewhat in contact with adjacent oxygen anions and proton transfer would be fast. However, strong hydrogen bonding is associated with more closely packed structures that have smaller separation between oxygen anions and stiffer B-O vibrations. It is likely that despite rapid proton transfer between oxygen anions in closely-packed hydrogen-bonded systems, reorientation of protons around the oxygen anions is slow and becomes rate limiting. Therefore, based on quantum molecular dynamics simulations, a compromise between the oxygen-oxygen separation and the stiffness of the B-O bonds must be achieved to maximize proton conductivity.[24,25] From these simulations, the calculated barrier for proton conduction was lower for $BaCeO_3$ than the more closely-packed $BaZrO_3$.[24,25] However, the stiffness of the Ti-O bond in $BeTiO_3$ was more optimally compensated by oxygen-oxygen separation, and $BaTiO_3$ was predicted to have the lowest barrier for proton conduction.[24,25]

CHEMICAL STABILITY OF PEROVSKITE-BASED MEMBRANES

Obviously high proton and electron conductivity is a prerequisite for the proposed materials to be used in commercially viable, however, adequate material stability also must be achieved. Unfortunately, the chemical qualities that lead to high charge carrier uptake also can lead to material degradation depending on the operating conditions. For example, introduction of proton charge carriers by moisture uptake is more favorable for $BaCeO_3$ relative to $SrCeO_3$ or $BaZrO_3$ due in part to the greater basicity of $BaCeO_3$.[4] However, the higher basicity of $BaCeO_3$ makes it more vulnerable to decomposition in the presence of moisture, as well as other acidic gases such as CO_2.[4] Specifically, it has been shown that $BaCeO_3$ doped with some rare earth oxides decomposes into $Ba(OH)_2$ and CeO_2 at water vapor pressures above 430 torr and temperatures less than 900°C.[26] Similarly, although La- and Gd-doped $BaCeO_3$ actually appear stable in water vapor at elevated temperatures, decomposition occurs when the temperature is reduced to 85°C, which could be problematic in applications where temperature cycling is necessary.[27] Furthermore, cerate-based perovskite materials generally appear stable in CO_2-containing environments over limited test periods; however, based on thermodynamic considerations it is unlikely that such materials would posses long-term stability outside of a narrow range of operating conditions.[4,14] Strategies for balancing high charge carrier uptake and proton mobility with adequate material stability are discussed below.

STRATEGIES FOR DEVELOPMENT OF HYDROGEN TRANSPORT MEMBRANES

During this project, Eltron and team members CoorsTek, McDermott Technology, Süd Chemie, Argonne National Laboratory, and Oak Ridge National Laboratory will be working to improve hydrogen transport through dense ceramic-based membranes. As summarized in Figure 2, the overall approach is divided into three categories: i) optimization of perovskite compositions for mixed proton and electron conductivity and stability, ii) development of multi-phase materials, and iii) fabrication of supported thin films. These areas represent three different strategies for improving membrane performance and address the primary technical obstacles for advancing gas separation membrane technology. A brief description of each category is presented below.

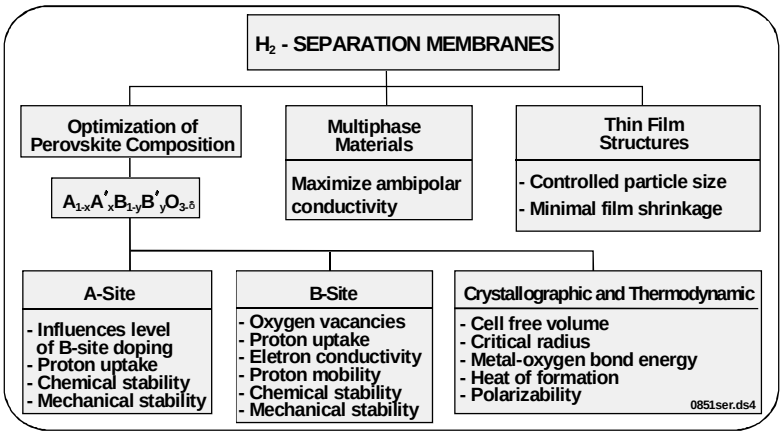

Figure 2. Summary of the strategy for development of hydrogen separation membrane technology.

Optimization of Perovskite Composition

Although there is considerable overlap in the material properties influenced by the A and B sites of the perovskite lattice, certain properties can be controlled more by selectively doping one site over the other. The B site cation has the greatest influence on proton conductivity and, therefore, the vast majority of published work in this area has focused on the influence of B site dopants. The cation in the B position has a 4+ charge, and electroneutrality is maintained by the A site cation and oxygen anions. Doping the B site with lower valence cations results in an excess of negative charge that is accommodated by formation of oxygen vacancies. Consequently, the concentration of oxygen vacancies is directly proportional to the level of B site doping. It was shown in Equations 1 through 4 that oxygen vacancies are partly responsible for uptake of protons, so high charge carrier concentrations in perovskite materials can be achieved by high levels of doping. Accordingly, one of the main objectives for material development during this program will be to maximize B site doping while maintaining the desired mixed conducting phase(s).

Incorporation of protons into the perovskite lattice can be viewed as acid/base chemistry, and the basicity of the B site (and A site) cation also will influence the proton concentration.[4] However, as indicated above, increased basicity can lead to reaction with moisture and CO_2 to produce the corresponding oxide, hydroxide, or carbonate, and this tendency can be anticipated from the enthalpy

of formation of the decomposition products.[4,26,27] For example, as a preliminary prediction of material stability the equilibrium partial pressures of CO_2 as a function of temperature were calculated for ten well-studied perovskite proton conductors with Ca, Sr, and Ba as A site elements, and Ti, Zr, Hf, and Ce as B site elements. The results are shown in Figure 3. The thermodynamic data for cerium related reactions were taken from references 28-30, and the rest of the data were taken from reference 31. In the figure, the line for each composition indicates the equilibrium partial pressure for CO_2, and a given material only will be thermodynamically stable at or below values on the line. From this preliminary group, the most CO_2-resistant material was $SrTiO_3$, and the least resistant was $BaCeO_3$.

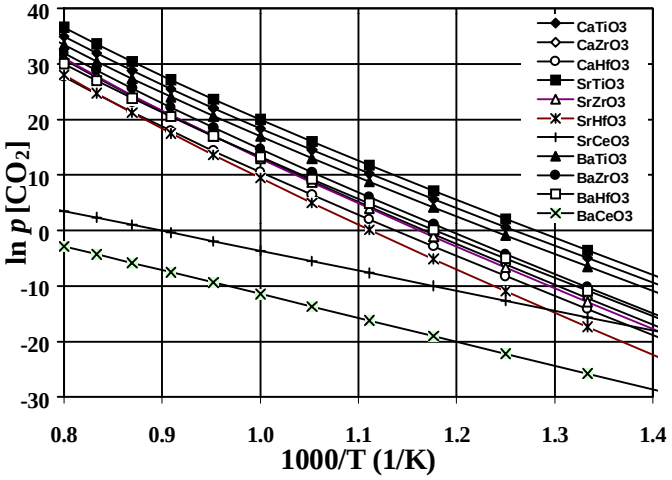

Figure 3. Plot demonstrating the stability of perovskite compositions as a function of CO_2 partial pressure and temperature.

Based on these considerations, a logical material development strategy for maximizing *proton* conductivity is to incorporate dopants for mixed B site basicity and achieve an optimum compromise between proton uptake and resistance to decomposition. Moreover, the identities of the B site cation and dopant will affect other relevant variables such as the rigidity of B-O bonding, the degree of hydrogen bonding, and the crystal packing density. Ultimately these factors affect proton mobility in the lattice, and should be considered when choosing candidate compositions. Mixed basicity of the B site should be accomplished with cations that produce loosely-packed structures and/or soft B-O vibrations.

The relationship between the B site cation and dopant controls electron conductivity as well as proton conductivity. Electron conductivity is a consequence of mixed valency within the B site and overlap of B site cation and oxygen orbitals according the Zerner double exchange process,

$$B^{n+}\text{-}O^{2-}\text{-}B^{(n+1)+} \leftrightarrows B^{n+}\text{-}O^{-}\text{-}B^{n+} \leftrightarrows B^{(n+1)+}\text{-}O^{2-}\text{-}B^{n+}. \quad (5)$$

The greater the B cation and oxygen orbital overlap, the more the electron conduction process is facilitated.[32,33] However, this scenario also suggests that maximizing the number of oxygen vacancies could suppress electron conduction. In fact, this trend has been observed for the mixed oxygen ion/electron conductor $La_{1-x}Sr_xCoO_{3-\delta}$.[34] In that work, the electrical properties were found to be independent of the number of Co 3*d* electrons, and determined by the concentration of oxygen defects.[34] The authors observed a clear reduction in conductivity upon increasing the number of oxygen vacancies, and reasoned that such defects distorted the CoO_6 octahedron and narrowed the conduction band.[34] Therefore, ceramic membrane development can not focus only on maximizing oxygen vacancies.

Although generally considered less interesting than the B site, there are several objectives for manipulating the perovskite A site. First, appropriately doping the A site can lead to an increase in the solubility range for B site doping. Support for this strategy is found in the literature for the oxide ion conductor $LaGaO_3$.[35] Controlling *both* the Sr doping on the A site and Mg doping on the B site led to a maximum oxide ion conductivity of 0.166 S/cm at 800°C for $La_{0.8}Sr_{0.2}Ga_{0.83}Mg_{0.17}O_{2.8}$.[35]

Furthermore, as with the B site, the basicity of the A site cation and dopant also affects the uptake of proton charge carriers and material stability. This factor has been used to partially explain the greater tendency of $BaCeO_3$ to hydrate relative to $SrCeO_3$.[4] Also, it has been demonstrated for Y-doped $BaCeO_3$ that a stoichiometric deficiency in the A site results in higher chemical stability.[37] Specifically, X-ray diffraction patterns for materials represented by $Ba_xCe_{0.9}Y_{0.1}O_{3-\delta}$ were followed for up to 150 days, and it was shown that for $x \geq 1$ significant levels of $BaCO_3$ were formed, and the intensity of $BaCO_3$ diffraction peaks increased with Ba content in the perovskite.[37S] Conversely, materials with $x < 1$ showed no evidence of $BaCO_3$ formation, and the maximum ionic conductivity actually was observed for $x = 0.95$.[37] Therefore, mixed basicity and stoichiometric deficiency in the A site both offer a potential strategy for composition optimization.

Development of Multi-Phase Materials

An alternative to single phase membranes is two-phase compositions where one phase is predominantly a proton conductor and the other phase is predominantly an electron conductor. The potential advantage of this approach is that conductivities of each phase can be optimized independently without concern over improving one quality at the cost of another. The major technical obstacle then becomes achieving compatibility of the two phases.

When both phases are percolative, hydrogen transport can be characterized by the ambipolar conductivity, σ_{amb}, given by the expression,

$$\frac{1}{\sigma_{amb}} = \frac{\tau_i}{f_i \sigma_i} + \frac{\tau_e}{f_e \sigma_e} \qquad (6)$$

where σ_i and σ_e are the ionic (proton) and electron conductivities, f_i and f_e are the volume fractions of the ion and electron conducting phases, and τ_i and τ_e are dimensionless geometric factors.[38] Accordingly, there exists an optimum volume fraction of each phase where σ_{amb} is maximized.

Optimum volume fractions can be predicted using percolation theory, which was first developed by Broadbent and Hammersley.[39] Percolation theory gives a phenomenological equation for the conductivity of a composite medium transition, such as a metal-insulator or perfect conductor-poor conductor. Although the theory was mainly developed in the context of regular lattices, it also is used to describe the conductivity of continuum systems, such as metal-ceramic and graphite-polymer mixtures. The central feature of percolation models is the percolation threshold where the effective transport coefficients change sharply from nonconducting to conducting behavior. An example is shown in Figure 4. Assuming phase 1 of the composite has high ionic conductivity, $\sigma_{i,1}$,

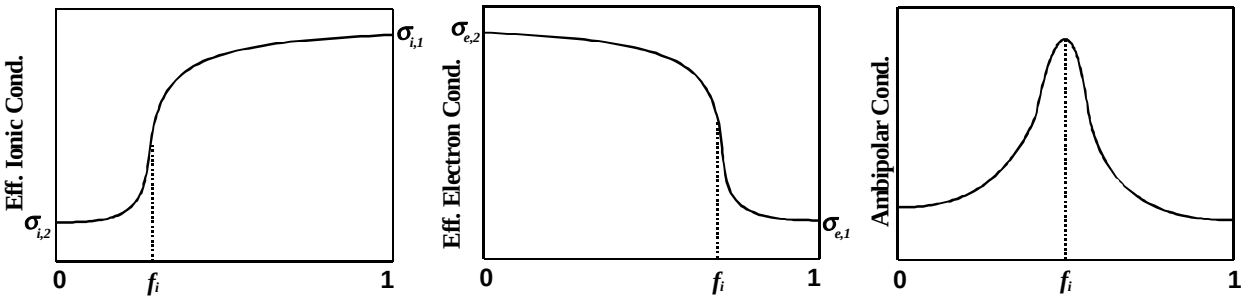

Figure 4. Diagram showing the relationship between effective ionic and electron conductivity, and the ambipolar conductivity as a function of composite volume fraction.

and low electronic conductivity, $\sigma_{e,1}$, and phase 2 has high electronic conductivity, $\sigma_{e,2}$, and low ionic conductivity, $\sigma_{i,2}$, such that $\sigma_{i,1} >> \sigma_{i,2}$ and $\sigma_{e,1} << \sigma_{e,2}$, then percolation theory can predict an effective ionic and electron conductivity of the composite. In the figure, f_i is the volume fraction of the ionic conducting phase (phase 1), and 1 - f_i is the volume fraction of the electron conducting phase (phase 2). Thus, when f_i is 0 the effective ionic conductivity is low and equal to $\sigma_{i,2}$, and the effective electron conductivity is high and equal to $\sigma_{e,2}$. As f_i increases, there is a sharp change in the effective ionic and electron conductivity of the material corresponding to the percolation thresholds of the two phases. The resulting σ_{amb} demonstrates a maximum for an optimum f_i, which is dependent on many factors, including particle size and shape of each phase, distribution of phases, and possible interactions between phases. Correspondingly, these factors potentially allow adjustment of the percolation thresholds through composite engineering to achieve the desired performance.

Supported Thin Film Membranes

Although conductivity is a material property, hydrogen flux, J, through the membrane in the absence of surface kinetic limitations will depend in part on the membrane thickness, t, according to,

$$J = \frac{\sigma_{amb} V}{t} \tag{7}$$

where V is the driving potential resulting from a hydrogen partial pressure gradient. Therefore, dramatic improvements in hydrogen separation rates can be achieved by producing supported thin membrane structures. Furthermore, practical transport rates likely can be attained with more stable membrane compositions.

Numerous methods have been investigated for thin film production,[40-53] and many of the technical obstacles were recently overcome by Souza *et al.* for production of dense thin films of yttria-stabilized zirconia (YSZ) for solid oxide fuel cell applications.[44,45] In their work, YSZ films between 4 and 10 μm thick were prepared from a colloid dispersion of 0.2-μm YSZ particles coated onto a porous Ni/YSZ cermet. Films were successfully prepared by carefully controlling shrinkage rates of the support and growing film. Control of the shrinkage rate was obtained through trial-and-error experimentation by varying parameters such as the metal oxide particle size used to prepare the substrate, the coarsening schedule, homogeneity and morphology of the substrate, and the binder and dispersant concentrations. Furthermore, problems associated with mismatch in thermal expansion

between the film and substrate were remedied by designing the supported film so that differences in expansion resulted in a net compressive strain on the YSZ film. The significance of the work by Souza *et al.* with regard to ceramic membranes is that metal oxide particles can be used to achieve very thin dense ceramic membranes. Moreover, the particle sizes used (0.2 μm) are easily achieved by attrition of conventionally-prepared metal oxide powders. Consequently, special techniques are not required for their preparation. The main drawback of this process is that it is system specific and the exact preparation variables need to be determined for different substrate/ceramic film combinations.

A polymeric precursor method attempts to provide a more general approach for preparing dense thin ceramic films.[48-53] Although many variations of the method exist, Agarwal and Liu recently prepared thin $BaCeO_3$-based films using ethylenediamine tetraacetic acid (EDTA) to chelate constituent metal cations in solution for the preparation of the film precursor.[49] Addition of ethylene glycol to the solution resulted in the formation of esters that were polymerized upon heating. This procedure was a modification of a process patented by Pechini,[54] and resulted in evenly distributed metal ions throughout the solution, tethered to the polymers. The desirable features of this process are as follows: i) it is not necessary to account for differences in metal solubilities in complex mixtures, ii) there is little formation of metal-oxygen-metal bonds prior to pyrolysis (which can lead to film cracking), iii) the metal cations remain evenly distributed throughout the solution until heating, which is critical for forming dense, nonporous, homogeneous coatings, iv) the polymeric precursor can flow easily over rough surfaces such as a porous substrate, v) upon heating, the precursor decomposes to form very fine particles that aid in adhering the coating to the substrate, and finally, vi) the process is simple, inexpensive, and generally applicable to a wide variety of metal cations, unlike sol gel processes which require expensive metal alkoxides and more complicated chemistry.

The major drawback of the polymeric precursor method is that the precursor gel is primarily organic, which leads to two problems. First, the loss of volume as the organic material decomposes leads to high shrinkage rates and cracking of the membrane film. Second, the gaseous decomposition products can produce "pinholes" in the membrane film. To circumvent this problem a two-phase sol gel based precursor has been described for the production of alumina films.[55] This precursor was composed of an aluminum *sec*-butoxide derived gel mixed with commercially available 0.32-μm alumina powder. This two-phase precursor resulted in much less shrinkage due to the alumina particles, and gel-facilitated binding between the alumina particles and the substrate.

Eltron has adapted key features of the above methods for production of oxygen separation membranes on the order of 10 μm thick. This modified technique also will be applied to fabrication of hydrogen separation membranes. Additionally, a novel tape casting process has been used to produce ~ 100-μm thick membranes that soon will be tested for hydrogen transport. A preliminary example is shown in Figure 5. The dense doped-perovskite film was supported on a porous disk of the same composition. The film was single phase and very homogeneous, showing no signs of cracks or other structural defects.

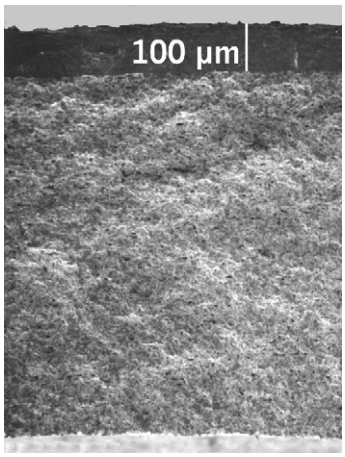

Figure 5. Scanning electron micrograph (cross section) of a thin perovskite film deposited onto a porous support.

SUMMARY OF PROJECT RESULTS

To date, highest mixed proton and electron conductivity at Eltron has been observed for multi-phase compositions containing a combination of a predominantly proton conducting phase and an electron conducting phase. Multi-phase ceramics and ceramic/metal (cermet) compositions demonstrate mixed conductivity (ambipolar) as high as 8 x 10^{-3} S/cm, with corresponding hydrogen separation rates between 0.01 and 0.3 mL/min/cm^2 for thick membranes (1.0 mm) at high temperatures (850°C). Hydrogen transport through ceramic membranes is dependent on the concentration and identity of transition metal dopants and metal oxides included in the composition. Similarly, hydrogen transport through cermet membranes is dependent on the ceramic phase composition, as well as the volume percent of the metal phase.

INCORPORATION INTO A VISION 21 FOSSIL FUEL PLANT

Exact membrane designs and separation vessel configurations will evolve as the technology matures. However, it is likely that the final design will consist of large arrays of membranes assembled into a series of individual modules, as has been proposed for porous membrane systems. A simplified block diagram of a hydrogen separation unit installed in an integrated gasification combined cycle (IGCC) plant is shown in Figure 6. Coal is gasified and filtered to produce clean syngas that passes through the hydrogen separation unit. The hydrogen-depleted syngas exiting the unit is combusted to power a gas turbine and generate electricity. The separated hydrogen is recovered, and heat from both the separation unit and gas turbine is recovered and converted to electricity using a steam turbine. The end result of this operation is clean production of electricity and pure hydrogen from an inexpensive contaminant-containing fuel source.

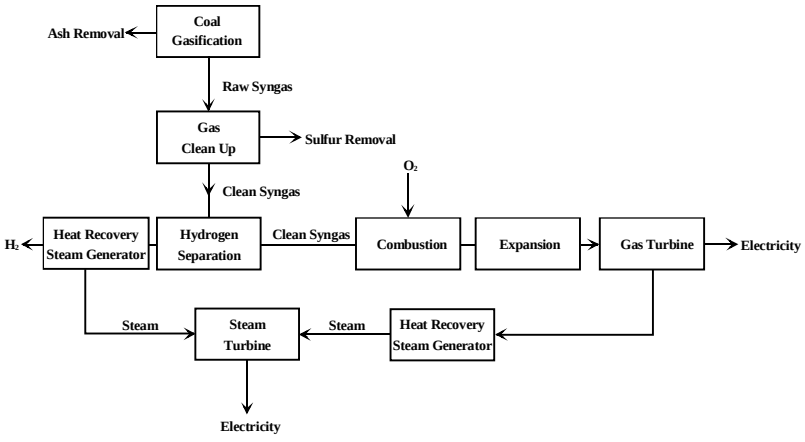

Figure 6. Schematic diagram demonstrating a hydrogen separation unit incorporated into an IGCC plant.

ACKNOWLEDGMENTS

Development of hydrogen separation membranes at Eltron Research, Inc. currently is funded by DOE/NETL under contract number DE-FC26-00NT40762.

REFERENCES

1. Iwahara, H.; Esaka, T.; Uchida, H.; Maeda, N. *Solid State Ionics* **1981**, *3/4*, 359.
2. Iwahara, H.; Uchida, H.; Ono, K.; Ogaki, K. *J. Electrochem. Soc.* **1988**, *135*, 529.
3. Lee, W.; Nowick, A. S. *Solid State Ionics* **1986**, *18/19*, 989.

4. Kreuer, K. D. *Solid State Ionics* **1997**, *97*, 1.
5. Bonanos, N.; Ellis, B.; Knight, K. S.; Mahmood, M. N. *Solid State Ionics* **1989**, *35*, 179.
6. Bonanos, N. *Solid State Ionics* **1992**, *53-56*, 967.
7. Bonanos, N. *J. Phys. Chem. Solids* **1993**, *54*, 867.
8. Iwahara, H.; Uchida, H.; Morimoto, K. *J. Electrochem. Soc.* **1990**, *137*, 462.
9. Shima, D.; Haile, S. M. *Solid State Ionics* **1997**, *97*, 443.
10. Norby, T.; Larring, Y. *Concentration and Transport of Protons and Oxygen Defects in Oxides*; Norby, T.; Larring, Y., Ed.; The Institute of Materials, 1996, pp 83-93.
11. Yajima, T.; Iwahara, H. *Solid State Ionics* **1992**, *50*, 281.
12. Liang, K. C.; Nowick, A. S. *Solid State Ionics* **1993**, *61*, 77.
13. Norby, T. *Solid State Ionics* **1990**, *40/41*, 857.
14. Bonanos, N.; Knight, K. S.; Ellis, B. *Solid State Ionics* **1995**, *79*, 161.
15. Balachandran, U.; Ma, B.; Maiya, P. S.; Mieville, R. L.; Dusek, J. T.; Picciolo, J.; Guan, J.; Dorris, S. E.; Liu, M. *Solid State Ionics* **1998**, *108*, 363.
16. Balachandran, U.; Guan, J.; Dorris, S. E.; Bose, A. C.; Stiegel, G. J. *Development of Mixed-Conducting Dense Ceramic Membranes for Hydrogen Separation*; Balachandran, U.; Guan, J.; Dorris, S. E.; Bose, A. C.; Stiegel, G. J., Ed.: Nagoya, Japan, 1998.
17. Roark, S. E.; White, J. H.; Sammells, A. F.; Dane, J.; Keeley, J. "Mixed-Conducting Membranes for the Spontaneous Oxidative Dehydrogenation of Alkanes to Olefins," Final Report, March 17, 1999, DOE Contract No. DE-FG0397ER82571,Eltron Research, Inc.
18. Kroger, F. A. *The Chemistry of Imperfect Crystals*; North Holland Publishing Co.: Amsterdam, 1964.
19. Iwahara, H.; Uchida, H.; Morimoto, K.; Hosogi, S. *J. Appl. Electrochem.* **1989**, *19*, 448.
20. Iwahara, H. *Solid State Ionics* **1992**, *52*, 99.
21. Iwahara, H.; Hibino, T.; Sunano, T. *J. Appl. Electrochem.* **1996**, *26*, 829.
22. Yajima, T.; Kazeoka, H.; Yoga, T.; Iwahara, H. *Solid State Ionics* **1991**, *47*, 271.
23. Kreuer, K. D.; Fuchs, A.; Maier, J. *Solid State Ionics* **1995**, *77*, 157.
24. Munch, W.; Seifert, G.; Kreuer, K. D.; Maier, J. *Solid State Ionics* **1996**, *86-88*, 647.
25. Munch, W.; Seifert, G.; Kreuer, K. D.; Maier, J. *Solid State Ionics* **1997**, *97*, 39.
26. Tanner, C. W.; Virkar, A. V. *J. Electrochem. Soc.* **1996**, *143*, 1386.
27. Bhide, S. V.; Virkar, A. V. *J. Electrochem. Soc.* **1999**, *146*, 2038.
28. Oknacke, O.; Kubaschewski, O.; Hesselmann, K. *Thermodynamic Properties of Inorganic Substances*; 2 ed.; Springer-Verlag: Berlin, Germany, 1991.
29. Sorokina, S. L.; Skolis, Y. Y.; Kovba, M. L.; Levitskii, V. A. *Russ. J. Phys. Chem.* **1986**, *60*, 186.
30. Levitskii, V. A.; Sorokina, S. L.; Skolis, Y. Y.; Kovba, M. L. *Inorg. Mater.* **1990**, *21*, 1990.
31. E.S. Microware, I. *Thermochemical and Physical Properties*; E.S. Microware, I., Ed., 1994.
32. Goodenough, J. B. *Prog. Solid State Chem.* **1971**, *5*, 149.
33. Goodenough, J. B. ; Marcel Dekker, Inc.: New York, 1974.
34. Mizusaki, J.; Tabuchi, J.; Matsuura, T.; Yamauchi, S.; Fueki, K. *J. Electrochem. Soc.* **1989**, *136*, 2082.
35. Huang, K.; Tichy, R. S.; Goodenough, J. B. *J. Am. Ceram. Soc.* **1998**, *81*, 2565.
36. Gopalan, S.; Virkar, A. V. *J. Electrochem. Soc.* **1993**, *140*, 1060.
37. Ma, G. L.; Shimura, T.; Iwahara, H. *Solid State Ionics* **1998**, *110*, 103-110.

38. Elshof, J. E. t.; Nguyen, N. Q.; Otter, M. W. d.; Bouwmeester, H. J. M. *J. Electrochem. Soc.* **1997**, *144*, 4361-4366.
39. Broadbent, S. R.; Hammersley, J. M. *Proc. Camb. Soc.* **1957**, *53*, 629.
40. Segal, D. *J. Mater. Chem.* **1997**, *7*, 1297.
41. Pal, U. B.; Singhal, S. C. *J. Electrochem. Soc.* **1990**, *137*, 2937.
42. Levi, C. G. *Acta Mater.* **1998**, *46*, 787.
43. Agarwal, V.; Liu, M. *J. Electrochem. Soc.* **1996**, *143*, 3239.
44. Souza, S. D.; Visco, S. J.; Jonge, L. D. D. *Solid State Ionics* **1997**, *98*, 57.
45. Souza, S. D.; Visco, S. J.; Jonghe, L. C. D. *J. Electrochem. Soc.* **1997**, *144*, L35.
46. Livage, J.; Beteille, F.; Roux, C.; Charty, M.; Davidson, P. *Acta Mater.* **1998**, *46*, 743.
47. Agrawal, A.; Cronin, J. P.; Zhang, R. *Solar Energy Materials and Solar Cells* **1993**, *31*, 9.
48. Chen, C. C.; Nasrallah, M. M.; Anderson, H. U. *J. Electrochem. Soc.* **1993**, *140*, 3555.
49. Agarwal, V.; Liu, M. *J. Electrochem. Soc.* **1997**, *144*, 1035.
50. Liu, M.; Wang, D. *J. Mater. Res.* **1995**, *10*, 3210.
51. Zanetti, S. M.; Longo, E.; Varela, J. A.; Leite, E. R. *Mater. Lett.* **1997**, *31*, 173.
52. Arima, M.; Kakihana, M.; Nakamura, Y.; Yashima, M.; Yoshimura, M. *J. Am. Ceram. Soc.* **1996**, *79*, 2847.
53. Tai, L. W.; Anderson, H. U.; Lessing, P. A. *J. Am. Ceram. Soc.* **1992**, *75*, 3490.
54. Pechini, M. P. *Method of preparing lead and alkaline earch titanates and niobates and coating method using the same to form a capacitor*; U.S.A., Patent No. 3,330,697, 1967.
55. Shaw, L.; Abbaschian, R. *J. Am. Ceram. Soc.* **1995**, *78*, 3376.